Digest Journal of Nanomaterials and Biostructures Vol. 18, No. 2, April - June 2023, p. 495 - 510

Hydrogen production from hydrolysis of $NaBH_4$-NH_3BH_3 composite catalyzed by porous spherical Co_3O_4

M. Yang[a], Y. C. Wu[a], Y. H. Liu[a], Z. H. Li[a], M. Cheng[a], C. L. Wu[b], W. Feng[a, c, d], W. T. Cai[e,f], X. L. Wang[a,c,d,*]

[a]*School of Mechanical Engineering, Chengdu University, Chengdu 610106, PR China*

[b]*Engineering Research Center of Alternative Energy Materials & Devices, Ministry of Education, Sichuan University, Chengdu 610065, PR China*

[c]*Sichuan Province Engineering Technology Research Center of Powder Metallurgy, Chengdu University, Chengdu 610106, PR China*

[d]*Institute for Advanced Study, Chengdu University, Chengdu 610106, PR China*

[e]*School of Materials and Energy, Guangdong University of Technology, Guangzhou 510006, PR China*

[f]*Guangdong Provincial Key Laboratory of Advanced Energy Storage Materials, South China University of Technology, Guangzhou 510006, PR China*

$NaBH_4$-NH_3BH_3 composite (xSB-AB, x is the molar ratio of SB to AB) has better hydrolysis performance than its monomer, but the hydrogen generation rate (HGR) and hydrogen yield (HY) are still not ideal at room temperature. In this work, a low cost and easily available commercial porous spherical Co_3O_4 was successfully used to catalyze the hydrolysis of xSB-AB composite. It was found that Co_3O_4 showed good catalytic performance for the hydrolysis of xSB-AB, and the HY and hydrogen release efficiency (HRE) of 4SB-AB/10 wt%Co_3O_4 at 40 ℃ reached 2,279.71 $mL \cdot g^{-1}$ and 89.13%, respectively.

(Receipt January 3, 2023; Accepted April 11, 2023)

Keywords: Hydrogen production, Hydrolysis, $NaBH_4$, NH_3BH_3, Co_3O_4

1. Introduction

The signing of The Paris Agreement has further strengthened the universal understanding of human society on climate change[1, 2]. The policy of "CO_2 emission peak" and "carbon neutrality" have promoted the optimization and adjustment of the energy industry structure. At the same time, development of clean energy and reduction of carbon emissions are key factors to promote the sustainable development of human society[3-5]. As a zero-carbon emission clean energy carrier, hydrogen is considered to be the most potential substitute for fossil fuels in the

* Corresponding author: wangxiaolian@cdu.edu.cn
https://doi.org/10.15251/DJNB.2023.182.495

future, and the development of economical and effective hydrogen supply technology has become the key issue for the commercialization of portable hydrogen source devices[6, 7].

At present, the main hydrogen storage method contains high pressure gaseous hydrogen storage, low temperature liquid hydrogen storage and solid storage hydrogen storage[8]. Among them, solid-state hydrogen storage is favored because of its unique economic and safety advantages. The materials commonly used for solid-state hydrogen storage include hydrogen storage alloys, metal-organic framework materials, nano-carbon materials and various hydrides. Hydride hydrogen storage is a hydrogen storage method that stores hydrogen in various hydrides such as LiH, NaH, MgH_2, CaH_2, AlH_3, $NaBH_4$, $LiBH_4$ and NH_3BH_3, which can be released by chemical reaction when needed[9-13]. Among them, sodium borohydride ($NaBH_4$, SB) and ammonia borane (NH_3BH_3, AB) have theoretical hydrogen storage densities of 10.7 wt% and 19.6 wt%, respectively, which are excellent hydrogen storage materials.

SB has high thermal stability, and its decomposition temperature in dry air is about 300 ℃[14]. The thermal stability of AB is poor, but its pyrolysis dehydrogenation also needs a reaction temperature of 70-200 ℃, the pyrolysis dehydrogenation rate is slow, and some toxic borane gases will be produced[15]. Compared with the harsh dehydrogenation conditions and high energy consumption of pyrolysis, the hydrolysis of SB and AB to produce hydrogen has the advantages of low reaction temperature, simple operation, safe and stable hydrogen production process[16, 17]. Equations (1) and (2) are chemical reactions equations of SB and AB hydrogen production by hydrolysis respectively[18, 19], which have theoretical hydrogen storage capacity up to 10.92 wt% (SB-2H_2O) and 9.04 wt% (AB-2H_2O) respectively. However, the HGR of SB and AB at room temperature is very slow. For example, the hydrogen release amount of SB after reacting with water for 1 hour at room temperature is only about 2.17 wt%[20], and their low HRE is regarded as the key obstacle to its commercial application[21].

$$NaBH_4+2H_2O\rightarrow NaBO_2+4H_2\uparrow \quad (1)$$

$$NH_3BH_3+2H_2O\rightarrow NH_4^++BO_2^-+3H_2\uparrow \quad (2)$$

In order to improve the hydrolytic hydrogen production performance of SB and AB, various catalytic materials have been studied extensively. It is found that catalysts based on noble metals Ru[22-24], Rh[25, 26], Pt[27, 28] and Pd[29-31] have excellent catalytic performance, but their large-scale use is limited by high cost and scarce earth reserves. Therefore, it is a tendency to accelerate the development and use of cheaper and effective non-noble metal based catalysts. Cobalt-based catalysts are favored by researchers due to their remarkable catalytic activity and abundant reserves, such as Co_3O_4[32-35], Co-B[36-38], Co-P[39, 40], Co-Cu[41], Co-Cu-B[42, 43] and Co nanoparticles[44, 45]. V.I. Simagina et al.[46] studied the catalytic performance of Co_3O_4 in the hydrolysis of $NaBH_4$ and NH_3BH_3, and proposed that cobalt boride formed in situ from Co_3O_4 under the action of aqueous $NaBH_4$ is a promising catalyst for the hydrolysis of $NaBH_4$ and NH_3BH_3. Wu et al.[47] prepared a supported catalyst CoO_x-PG and CoO_x-GCNFs by loading Co_3O_4 on graphene materials (porous graphene and carbon nanofiber anchored graphene oxide). Due to the synergistic effect of Co_3O_4 and graphene, an outstanding catalytic effect was produced on the

hydrolysis of $NaBH_4$. The HGR of CoO_x-PG and CoO_x-GCNFs at room temperature can reach 1,472 $mL \cdot min^{-1} \cdot g_{co}^{-1}$ and 2,696 $mL \cdot min^{-1} \cdot g_{co}^{-1}$, respectively. Liu et al.[48] prepared a Co-based catalyst by wet chemical reduction method can effectively promote the hydrolysis of $NaBH_4$, and the further study found that the chemical composition of the catalyst surface is mainly cobalt oxide. Feng et al.[49] found that the catalytic performance of catalyst for AB hydrolysis changed significantly by regulating the proportion of metal in CoCu bimetallic oxide, which was due to by the change of electronic structure between metals in different proportions of CoCu. N.V. Lapin et al.[50] studied the feasibility of transition metal oxides such as cobalt and iron as catalysts for hydrogen production by AB hydrolysis, and found that the apparent activation energy pair of Co_3O_4 was 47.5 $kJ \cdot mol^{-1}$, indicating that the reaction could be carried out at room temperature.

In order to solve the problem of slow HGR of SB and AB monomers, we proposed the hydrolytic hydrogen production scheme of SB-AB composite[20, 51]. The results show that SB-AB composite has better hydrolysis performance than monomer, but its HGR and HY are still not ideal at room temperature. In order to improve the hydrolysis performance of SB-AB at room temperature, it is necessary to find a suitable catalyst. Our previous studies have shown that $AlCl_3$ has a definite catalytic performance for the hydrolysis of SB-AB, but the hydrogen yield is still low at room temperature. The maximum HY of SB-AB is only 1,875 $mL \cdot g^{-1}$ after 60 min reaction at 35 °C[52]. At present, cobalt-based catalysts are favored by researchers because of their remarkable catalytic activity and abundant reserves. Among the abundant cobalt-based catalysts, Co_3O_4 has been widely studied and used as a catalyst due to its advantages of stability, low cost and wide source[34]. At the same time, Co_3O_4 is insoluble in water and has magnetic properties, which make it easy to recover after the hydrolysis experiment.

In this work, low-cost and readily available commercial porous spherical Co_3O_4 was used to catalyze the hydrogen production from hydrolysis of SB-AB, and its hydrogen production behavior under different conditions was investigated by using the control variable method. The results show that the 4SB-AB/10 wt%Co_3O_4 reaction system has the favorable hydrogen production performance. Finally, the activation energy of the reaction was 59.12 $kJ \cdot mol^{-1}$ calculated by Arrhenius formula and hydrogen production curve at different temperatures. The SB-AB catalyzed by porous spherical Co_3O_4 may provide an efficient and convenient method for the design and development of solid hydrogen storage and release materials.

2. Experiment

2.1. Materials

In this experiment, Co_3O_4 (99.5%), $NaBH_4$ (98.0%) and $(NH_4)_2SO_4$ (97.0%) were purchased from Chengdu City Cologne Chemical Co., Ltd. All reagents were analytically pure and used directly without further processing. NH_3BH_3 was synthesized by $NaBH_4$ and $(NH_4)_2SO_4$ as raw materials. NH_3BH_3 was synthesized by the method mentioned in the literature with a purity of about 90%[53].

2.2. Preparation of hydrolysis raw materials

The hydrolysis raw materials (xSB-AB/yCo_3O_4, x is the molar ratio of SB to AB, y is the weight percentage of Co_3O_4) was prepared by two different Co_3O_4 addition methods. The addition method of mixing predetermined amount of pure SB, AB and Co_3O_4 by ball milling was defined as ball milling addition method. The direct addition method was defined as adding a certain amount of Co_3O_4 directly into xSB-AB prepared by ball milling in advance. The ball milling of SB-AB and xSB-AB/yCo_3O_4 was carried out by omnidirectional planetary ball milling (QM-QX, Nanjing Nanda Instrument Co., Ltd.) under argon atmosphere, the ball milling time was 15-60 min, and the weight ratio of ball material was 30:1[51]. All involving sample loading, sampling and sample transfer experiments were performed in a glove box (Model: DelliX-5611101) where the argon gas was 99.9% pure, with O_2 content < 1 ppm and H_2O content < 1 ppm.

2.3. Hydrolysis experiments and hydrolysate product collection

The experimental apparatus for testing the hydrolysis performance of xSB-AB/yCo_3O_4 reactants has been mentioned in previous work[20]. First, 0.2 g of the composite with different components was placed in a round-bottom flask and the round-bottom flask was placed in a constant temperature water bath. Secondly, after checking the air-tightness of the hydrolysis device, turn on the stirring device and condensate water, and inject a certain volume of deionized water into the round-bottom flask through the CTN-TCI-V microinjection pump at the injection rate of 100 $mL \cdot h^{-1}$. When the reaction begins, the generated gas passes through a solution of $CuSO_4$, a condensing tube, and a drying tube with $CaCl_2$. The function of these components was to absorbing ammonia in the gas, reducing the temperature of the gas and absorbing the water vapor emitted by the reaction to dry the gas, thus reducing experimental errors. Finally, the generated hydrogen was collected and measured in a 1.5 L inverted measuring cylinder filled with water (the measuring cylinder was immersed in the water tank at all times). Also, repeat each test at least three times to make ensure the accuracy of the results, and all the recorded hydrogen volumes were converted to the volume at 25 °C using the ideal gas equation.

After the hydrolysis experiment, the product in the round-bottom flask were collected and filtered in air to obtain black precipitation and transparent solution. The black precipitate and transparent solution were dried in a vacuum drying oven to obtain black powder and viscous crystallize product.

2.4. Characterization

The crystal structure of the material was analyzed by X-ray diffractometer (XRD, DX-2700B, Liaoning Dandong Haoyuan Instrument Co., Ltd.). The test conditions were as follows: CuKα radiation, graphite monochromator, step scanning mode, step Angle 0.06°, sampling time 0.5 s, tube voltage 40 kV, tube current 30 mA, the scanning range is 10~90°. The morphologies and microstructures of the material was analyzed by emission scanning electron microscope (SEM, FEI Inspect F50, Thermo Fisher Scientific Corporation).

3. Results and discussion

3.1. Organizational structure of hydrolysis raw materials

Fig. 1a shows the XRD patterns of xSB-AB (after ball milling, x=2, 4, 6 and 8) with different mole ratio of SB and AB after ball milling for 15 min in an argon atmosphere. The results of XRD analysis showed that the main phase of the xSB-AB was still $NaBH_4$ (JCPDS NO. 09-0386) and NH_3BH_3 (JCPDS NO. 13-0292), and no new phase was detected, indicating that there was no chemical change between SB and AB during ball milling. At the same time, it can be observed that with the increase of the mole ratio of SB-AB, the peak of AB gradually weakens, which was caused by the decrease of AB content. XRD data in Fig. 1b shows that XRD peaks of purchased Co_3O_4 were consistent with those of standard PDF cards (JCPDS NO. 42-1647), indicating that there is no quality problem with purchased Co_3O_4.

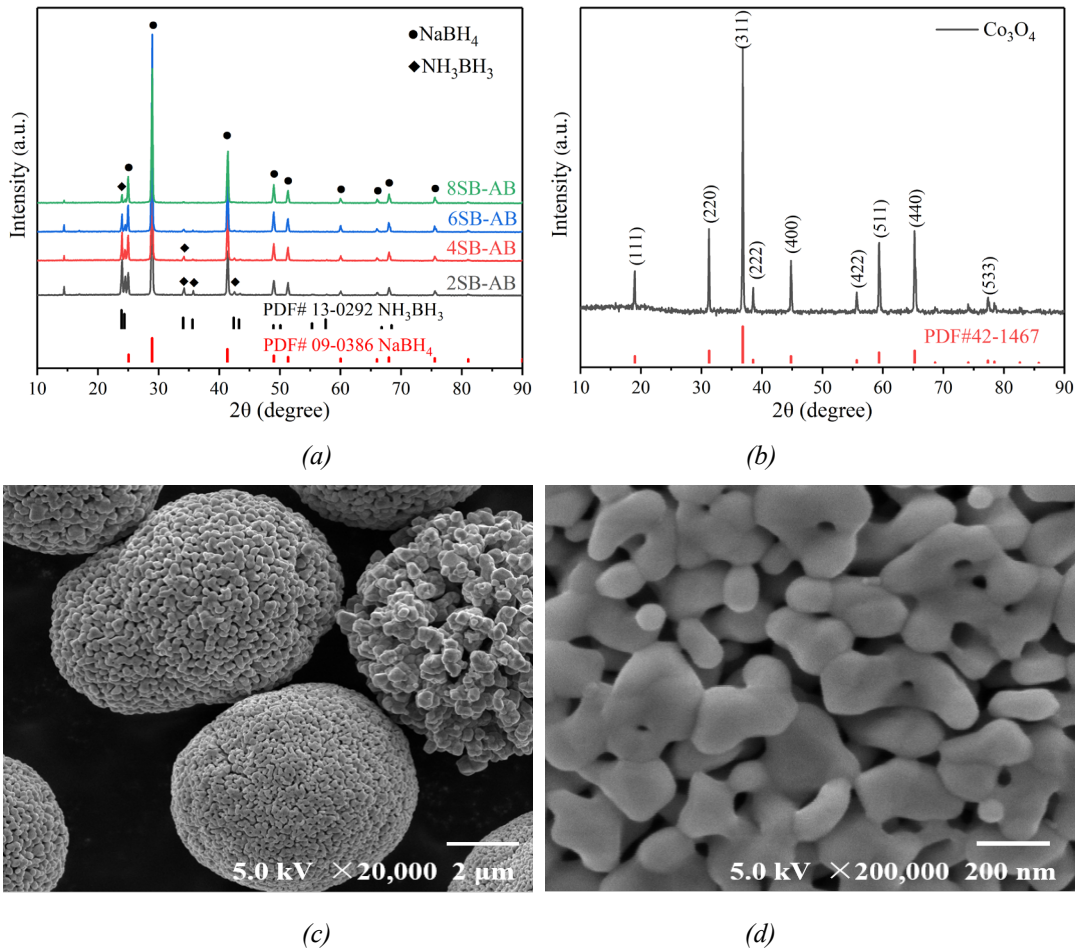

Fig. 1. XRD patterns of (a) xSB-AB (after ball milling, x = 2, 4, 6 and 8) and (b) Co_3O_4, SEM images of (c-d) Co_3O_4 catalyst.

Meanwhile, SEM analysis results further showed that the morphology of purchased Co_3O_4 showed a porous spherical structure, and its size was mainly distributed in the range of 5-7 μm (as shown in Fig. 1c-d). The surface of spherical Co_3O_4 was randomly distributed with pore structures of different sizes. The existence of these pore structures can significantly increase the specific surface area of Co_3O_4, which was conducive to increasing the area of contact with the reactants in the catalytic reaction process and accelerating the reaction. In addition, previous studies have shown that the size of pure SB particles without ball milling is mainly concentrated in the range of 200-500 μm, and the size of SB particles can be significantly reduced after ball milling[51]. Based on the above situation, the Co_3O_4 with porous spherical structure and the reactants with refined particle size will have more contact opportunities in the reaction process, which is conducive to the smooth progress of the reaction.

3.2. Hydrogen production performance

Our previous studies have shown that the hydrolysis of 4SB-AB generally has better hydrogen production performance than other xSB-AB (x=2, 4, 6 and 8)[51, 52].

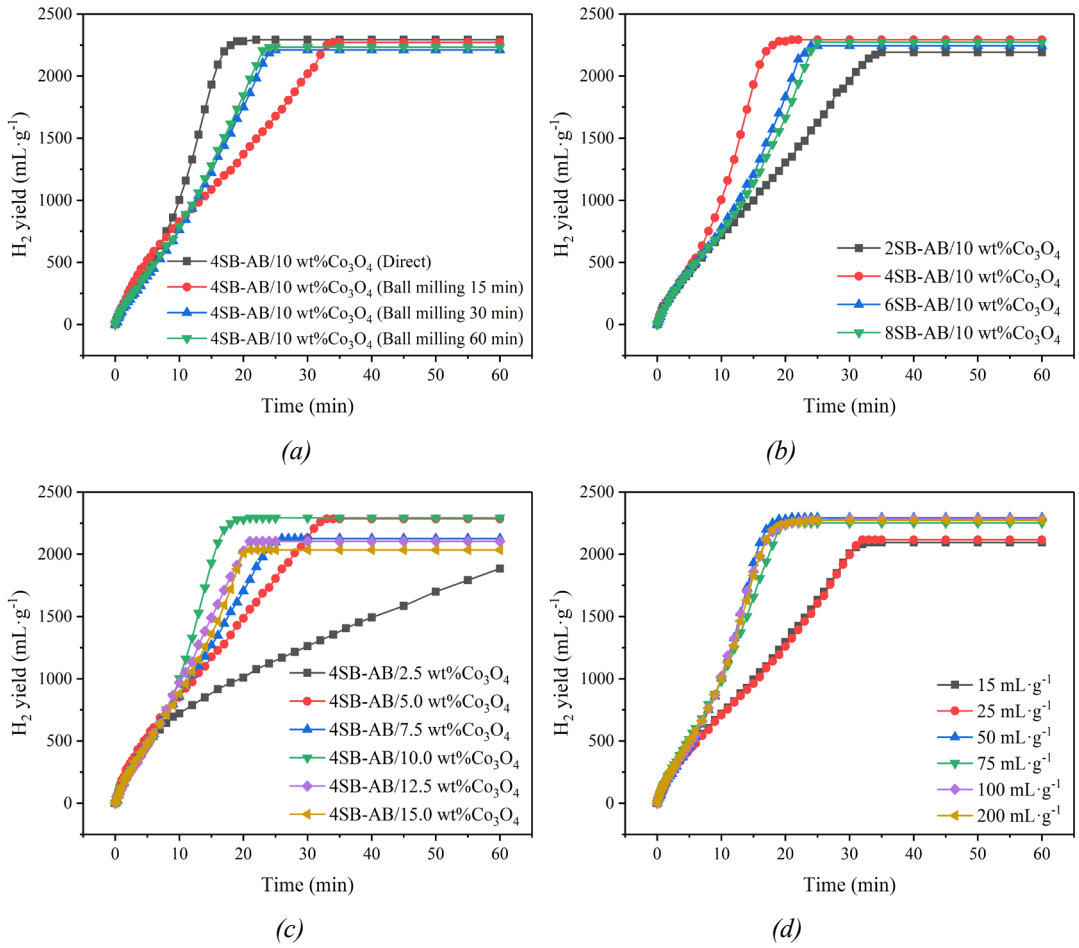

Fig. 2. The effect of (a) addition method of Co_3O_4, (b) molar ratio of SB to AB, (c) addition amount of Co_3O_4 and (d) ratio of water to material on the hydrogen production performance of xSB-AB/yCo_3O_4 hydrolysis. The reaction temperature was 40 ℃ (a-d), and the ratio of water to material was 50

mL·g^{-1} (a-c).

Therefore, 4SB-AB was used as the initial object for the study of SB-AB hydrolysis catalyzed by Co_3O_4, and the effect of Co_3O_4 addition method on the hydrolysis performance of 4SB-AB was investigated. Fig. 2a shows the effect of the addition method of Co_3O_4 on the hydrogen production performance of 4SB-AB/10 wt%Co_3O_4. It can be seen from Fig. 2a that under the same Co_3O_4 addition amount y (10 wt%), the HY and HGR of the composite obtained by direct addition of Co_3O_4 are significantly better than that obtained by ball milling. This may be because the catalyst distribution in the composite obtained by direct addition of Co_3O_4 is uneven, and the reaction in the small region where SB-AB is in full contact with Co_3O_4 will release concentrated heat[54], thus accelerating the reaction. Therefore, 4SB-AB/10 wt%Co_3O_4 obtained by direct addition of Co_3O_4 was selected to study the effect of molar ratio of SB to AB on the hydrogen production performance.

Our previous work has shown that the ratio of SB to AB has an important impact on the hydrogen production performance from hydrolysis of SB-AB[51]. Therefore, we investigated the effect of the molar ratio of SB to AB on the hydrogen production performance of SB-AB/10 wt%Co_3O_4. Fig. 2b shows the hydrogen production performance of xSB-AB/10 wt%Co_3O_4 (x=2, 4, 6 and 8). It can be seen from Fig. 2b, when the molar ratio of SB to AB increases from 2 to 8, the HGR of xSB-AB/10 wt%Co_3O_4 increased first and then decreased, shows a non-linear trend. Among them, 4SB-AB/10 wt%Co_3O_4 showed the favorable hydrogen production performance, with HY and HGR of 2,279.71 mL·g^{-1} and 119.98 mL·min^{-1}·g^{-1}, respectively. When x=2, 6, 8, here was little difference in HY of the composite, the HY were 2,192.81, 2,244.53 and 2,273.19 mL·g^{-1}, respectively. Therefore, 4SB-AB/10 wt%Co_3O_4 was selected to study the effect of Co_3O_4 addition amount on the hydrogen production performance.

Fig. 2c shows the hydrogen production performance of 4SB-AB/yCo_3O_4 (y = 2.5, 5.0, 7.5, 10, 12.5 and 15 wt%). It can be seen that when the addition amount of Co_3O_4 increased from 2.5 wt% to 15 wt%, the HGR of the 4SB-AB/yCo_3O_4 showed a non-linear trend (first increase and then decrease), and the HY showed an overall decreasing trend. This indicates that too much or too little amount of catalyst will affect the catalytic hydrogen release rate, which may be because the increase of catalyst addition content reduces the proportion of reactants. It may also be that under the condition of excessive catalyst addition, there is not enough reactant to fully contact with the catalyst. When Co_3O_4 content was 10 wt%, 4SB-AB/10 wt%Co_3O_4 exhibited the favorable hydrogen production performance, and had the fastest HGR (120.0 mL·min^{-1}·g^{-1}) and higher HY (2,279.71 mL·g^{-1}). Therefore, 4SB-AB/10 wt%Co_3O_4 was selected to study the effect of ratio of water to material and reaction temperature the hydrogen production performance.

Fig. 2d shows the effect of ratio of water to material (15, 25, 50, 75, 100 and 200 mL·g^{-1}) on the hydrogen production performance of 4SB-AB/10 wt%Co_3O_4. When the ratio of water to material was 50, 75, 100 and 200 mL·g^{-1}, there was little difference in the hydrogen production performance from hydrolysis of the 4SB-AB/10 wt%Co_3O_4. However, when the ratio of water to material was 15 and 25 mL·g^{-1}, the HGR and HY of the 4SB-AB/10 wt%Co_3O_4 decreased significantly. This is because when the content of water in the reaction is small, the contact degree between the composite and water is not sufficient and the reaction cannot be carried out

completely. When the contact between catalyst and reactant reached saturation state with the increase of ratio of water to material, the catalytic performance does not improve obviously. At the same time, the comparative analysis of Fig. 2a-d showed that there was no significant difference in the hydrogen production within 5 min before the reaction, because the content of water was relatively small at the beginning of the reaction and reaction could not be fully carried out. Combined with the above analysis results, too little ratio of water to material can significantly reduce the catalytic hydrogen release rate, while too much ratio of water to material has no obvious improvement in catalytic performance and increases the cost to a certain extent. The results show that the ratio of water to material of 50 $mL \cdot g^{-1}$ was the favorable choice for the 4SB-AB/10 wt%Co_3O_4.

3.3. Activation energy (E_a) of the reaction

It is well known that temperature is an important factor affecting the performance of the reaction. Therefore, the effect of reaction temperature on the hydrolysis performance of SB-AB was investigated. Fig. 3a and Table 1 shows the effect of reaction temperatures (10, 20, 30, 40, 50, 60 and 70 °C) on the hydrogen production performance of 4SB-AB/10 wt%Co_3O_4. It can be seen from Fig. 3a that with the increase of reaction temperature, the higher the initial reaction rate, the higher the HGR. The reason why the composite exhibits the excellent performance of hydrogen production by hydrolysis at high temperature is that with the increase of hydrolysis temperature, the more intense the movement degree of particles in the solution is, the more favorable it is to start and proceed the hydrolysis reaction. Although the hydrogen production performance at high temperature is significantly improved, the hydrolysis reaction at 30 °C also has good performance compared with the reaction at room temperature. These results indicate that Co_3O_4 catalyst can improve the hydrolysis performance of the SB-AB at room temperature to a certain extent.

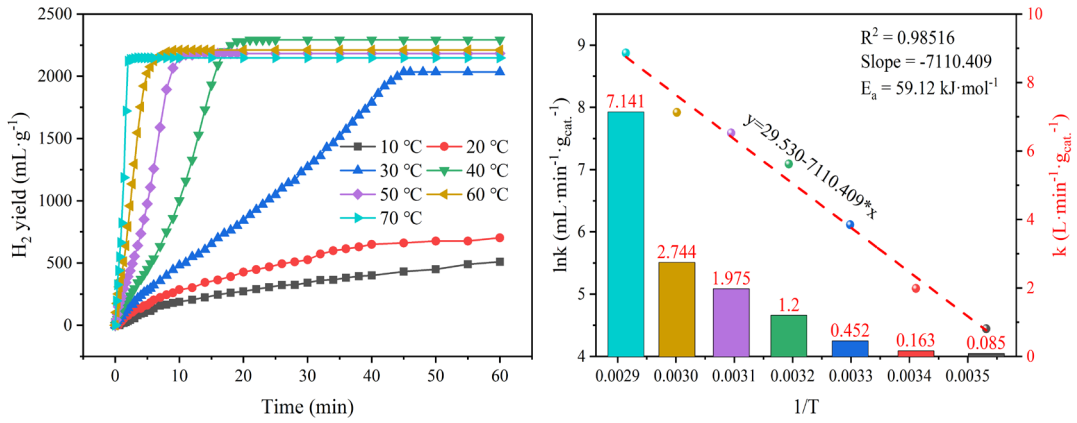

Fig. 3. (a) The effect of reaction temperature on the hydrogen production performance of 4SB-AB/10 wt%Co_3O_4, (b) Arrhenius plot (ln k versus reciprocal absolute temperature 1/T) and HGR values for hydrolysis reaction of 4SB-AB/10 wt%Co_3O_4.

Table 1. HY, HGR and HRE of composite with different of temperature.

Temperature/(℃)	10	20	30	40	50	60	70
HY/(L·g^{-1})	510.27	650.01	2,034.37	2,279.71	2,172.76	2,195.33	2,142.32
Reaction time/(min)	60	40	45	19	11	8	3
HGR/(mL·min^{-1}·g^{-1})	8.50	16.25	45.21	119.98	197.52	274.42	714.11
HRE/(%)	19.95	25.41	79.54	89.13	84.95	85.53	83.76

Note: HGR = HY/Reaction time, HRE = Actual hydrogen yield/Theoretical hydrogen yield.

Table 2. Comparison of the activation energy of various catalysts.

Catalyst	Reactants	Activation energy test		Reference
		RT/(℃)	E_a/(kJ·mol^{-1})	
Co-Cr-B/CeO_2	2.5 wt%$NaBH_4$ + 3 wt%NaOH	30-60	35.52	[55]
Co-Mo-B/NF	NH_3BH_3 solution	25-45	45.5	[56]
Co-Cr-B/γ-Al_2O_3	0.31 wt%NH_3BH_3 + 3 wt%NaOH	30-60	56.06	[57]
Co/NF	~3.8 wt%$NaBH_4$ + 4.5 wt%NaOH	25-40	60 ± 2	[58]
Co/γ-Al_2O_3	1 wt%NH_3BH_3	20-40	62	[59]
Co-B	20 wt%$NaBH_4$ + 5 wt%NaOH	10-30	64.87	[60]
Co/IR-120	5 wt%$NaBH_4$ + 5 wt%NaOH	20-50	66.67	[48]
Co_3O_4	4SB-AB/10 wt%Co_3O_4	10-70	59.12	This work

Note: RT, Reaction temperature; E_a, Activation energy; NF, Nickel foam.

In addition, under the catalytic action of Co_3O_4, the rate of hydrolysis of SB-AB at various reaction temperatures showed a linear relationship with the reaction time, this means that the reaction is of "zero order"[61]. Therefore, Arrhenius equation (Equations (3)) can be used to determine the activation energy (E_a) of the reaction[61-65]. The Arrhenius plot (lnk versus reciprocal absolute temperature 1/T) and HGR values for hydrolysis reaction of 4SB-AB/10 wt%Co_3O_4 are shown in Fig. 3b. Arrhenius plot showed that the E_a of 4SB-AB/10 wt%Co_3O_4 are 59.12 kJ·mol^{-1}. Compared with other Co-based catalysts (as shown in Table 2), the reaction E_a was relatively low, indicating that 4SB-AB/10 wt%Co_3O_4 had ideal hydrogen release kinetics.

$$k = A\exp(-E_a/RT) \quad (3)$$

3.4 Hydrolysate product analysis

Fig. 4a-b shows the XRD patterns of black powder, Co_3O_4 catalyst and viscous crystallize product. XRD data in Fig. 4a shows that the black powder was mainly composed of Co_3O_4 (JCPDS NO. 42-1467), and it also contains a certain amount of $Na_2B_2O_4 \cdot 8H_2O$ (JCPDS NO. 09-0011 and 14-0677), $NaBH_4 \cdot 2H_2O$ (JCPDS NO. 36-1233) and NaOH (JCPDS NO. 45-0744). This indicated that Co_3O_4 catalyst did not participate in

the reaction during the hydrolysis process, and could be recycled after the hydrolysis experiment. XRD data in Fig. 4b shows that the viscous crystalline product was mainly composed of $Na_2B_4O_7 \cdot 5H_2O$ (JCPDS NO. 07-0277) and $Na_2B_4O_7$ (JCPDS NO. 29-1179 and 51-1715), and it also contains a certain amount of BN (JCPDS NO. 25-1033 and 45-0895) and NaOH (JCPDS NO. 45-0744).

In order to further analyze the composition of the hydrolysate product, EDS was used to detect and analyze the elements of the black powder and viscous crystallize product, and the results were shown in Fig. 4c-f. EDS data in Fig. 4c-d show that the black powder contains Co, O, Na and N elements, among which O and Co have strong diffraction peaks. Combined with XRD analysis results, it can be seen that the main component of the black powder is Co_3O_4. Similarly, EDS and XRD results of viscous crystalline product show that its main component is borate. In addition, the elemental surface scanning (SEM mapping) results of black powder showed that the main elements were still Co and O (as shown in Fig. 4g), which were consistent with the elemental point scanning results (Fig. 4d).

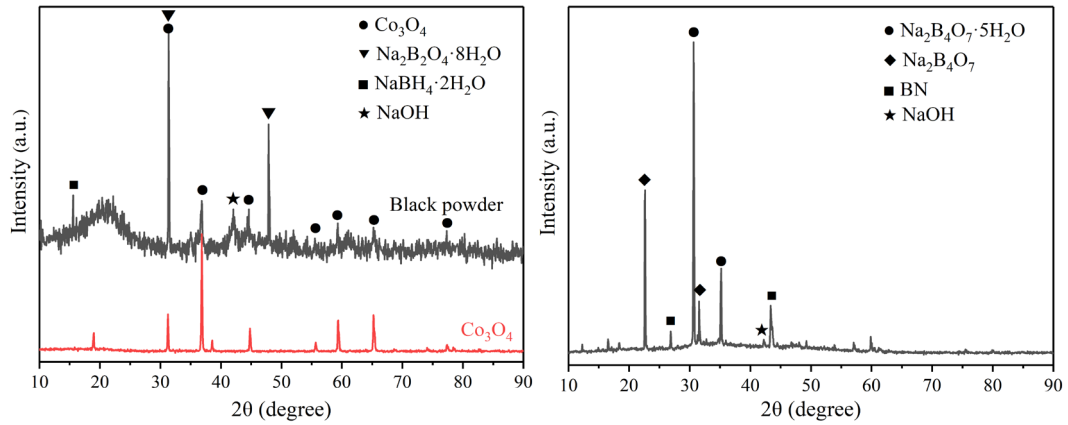

(a) *(b)*

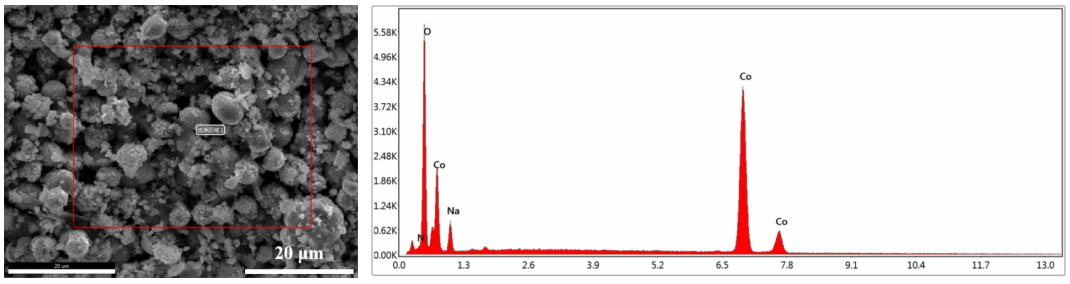

(c) *(d)*

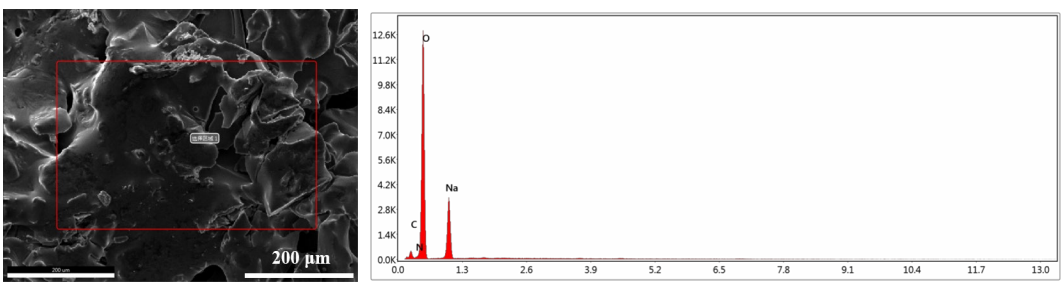

(e) *(f)*

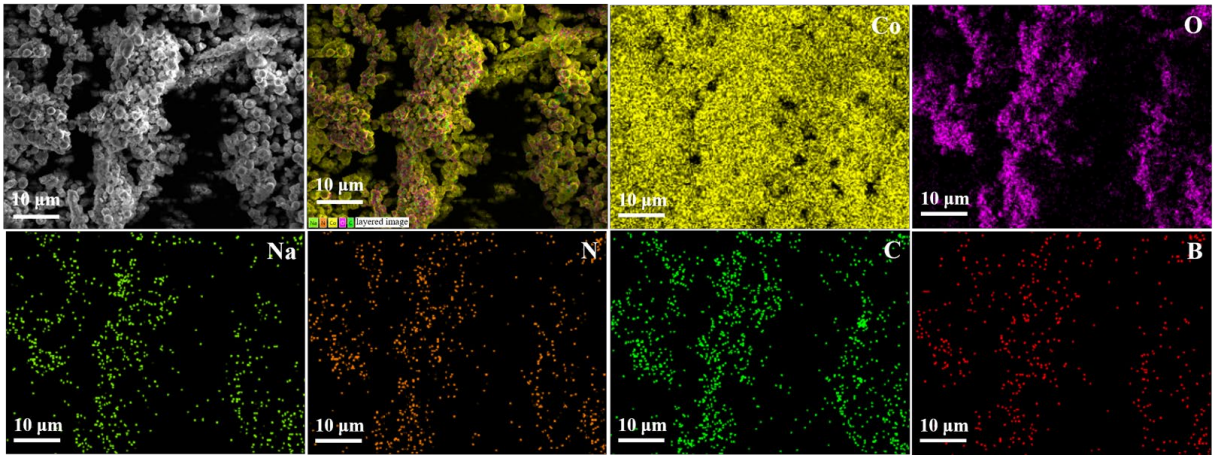

(g)

Fig. 4. XRD patterns of (a) black powder, Co_3O_4 catalyst and (b) viscous crystallize product; EDS results of (c-d) black powder and (e-f) viscous crystalline product; (g) SEM mapping of black powder.

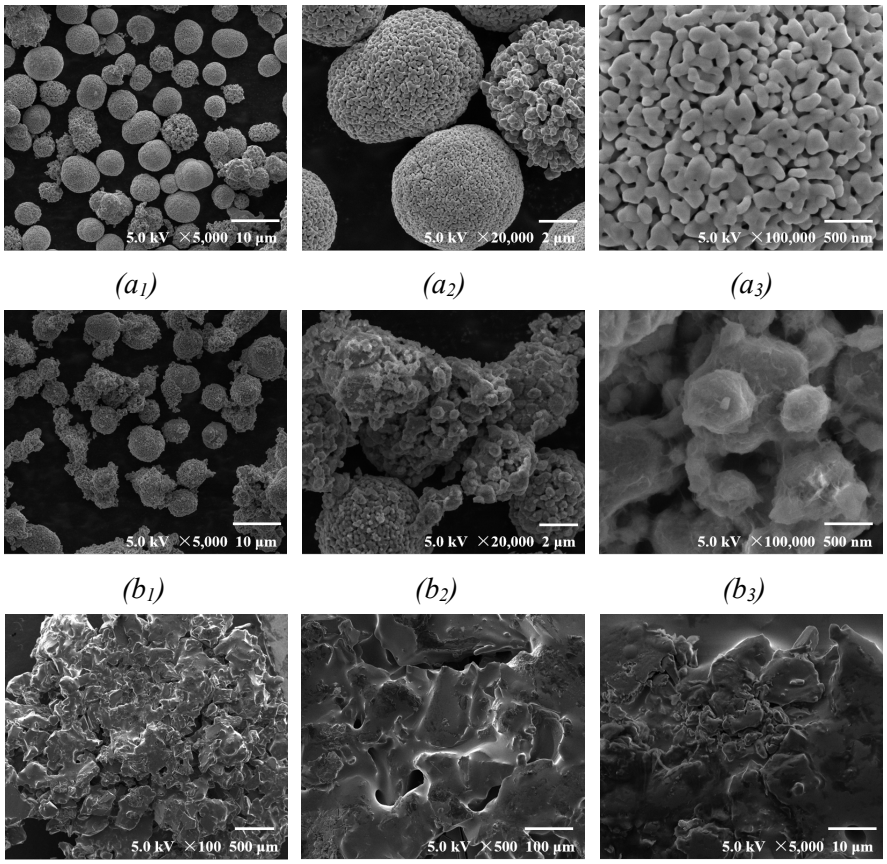

(a_1) *(a_2)* *(a_3)*

(b_1) *(b_2)* *(b_3)*

(c_1) *(c_2)* *(c_3)*

Fig. 5. SEM images of (a_1-a_3) purchased Co_3O_4, hydrolysate product (b_1-b_3) black powder and (c_1-c_3) viscous crystallization product.

In order to further explore the distribution of metaborate in the black powder and the reasons for its existence, SEM analysis was conducted on the black powder and the viscous crystalline product respectively, and the SEM images were compared with those of purchased Co_3O_4 (as shown in Fig. 5). Obviously, substances such as metaborate generated after hydrolysis reaction are adsorbed on the surface of Co_3O_4, leading to a certain degree of agglomeration of Co_3O_4 catalyst, and the pore structures on the surface of spherical Co_3O_4 are also covered. Fig. 6 shown in the schematic diagram of catalytic hydrolysis of xSB-AB by Co_3O_4 and the gradual surface atomization process of Co_3O_4 during the reaction process. From Fig. 6, we can intuitively see the contact level between xSB-AB and Co_3O_4 catalyst and the surface morphology of different reaction stages. With the progress of the reaction, metaborate is gradually coated on the surface of the Co_3O_4 catalyst (as shown in the second picture of Fig. 6), which also hinders contact between xSB-AB and Co_3O_4 catalyst to a certain extent. At the ending of the reaction SEM observed that the Co_3O_4 catalyst was agglomerated and atomized layer appeared on the surface (as shown in Fig. 5b_1-b_3). Therefore, the presence of metaborate in the recovered black powder is normal. As for the viscous crystalline product, no special morphology was found except the poor electrical conductivity during SEM shooting.

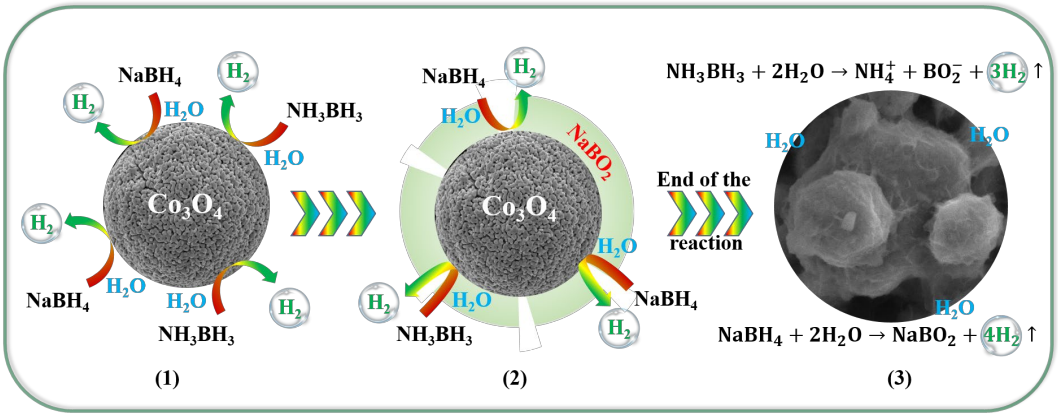

Fig. 6. Schematic diagram of catalytic hydrolysis of xSB-AB by Co_3O_4 and the gradual surface atomization process of Co_3O_4 during the reaction process.

4. Conclusion

The hydrolytic behavior of xSB-AB/yCo_3O_4 was studied in this paper. The hydrogen production performance of the composite was systematically studied from the addition method of Co_3O_4, the molar ratio of SB to AB, the addition amount of Co_3O_4, and the ratio of water to material. At the same time, the hydrogen production behavior of xSB-AB catalyzed by Co_3O_4 was discussed from hydrolysate product analysis and activation energy fitting calculation. The experimental results show that the hydrogen production performance of 4SB-AB directly added with Co_3O_4 is better than that of ball milling addition, and the metaborate produced by the reaction will be gradually coated on the surface of Co_3O_4 catalyst. When the ratio of water to material was

50 mL·g^{-1} and the reaction temperature was 40 ℃, the HY of 4SB-AB/10 wt%Co_3O_4 was up to 2,279.71 mL·g^{-1} and the average HGR of 119.98 mL·min^{-1}·g^{-1} (19 min before the reaction). The activation energy of the reaction was 59.12 kJ·mol^{-1}. These results indicate that the catalytic of SB-AB hydrolysis by Co_3O_4 is a feasible method and can be used in practical applications.

Acknowledgments

This work was supported by the Open Fund of Engineering Research Center of Alternative Energy Materials & Devices (grant number AEMD202203); the Chengdu University Talent Engineering Research Start-up Project (grant number 2081921083), the National Natural Science Foundation of China (grant number. 21805046, 22179024), the Science and Technology Plan Project of Guangzhou City (grant number 202102020426), the Open Fund of the Guangdong Provincial Key Laboratory of Advanced Energy Storage Materials, South China University of Technology (grant number AESM202111), Project of "One-Hundred Young Talents" of Guangdong University of Technology (grant number 220413551).

References

[1] Y. Robiou du Pont et al. Nature Climate Change 7(1), 38 (2016); https://doi.org/10.1038/nclimate3186

[2] J. Rogelj et al. Nature 534(7609), 631 (2016); https://doi.org/10.1038/nature18307

[3] M.-T. Huang et al. Advances in Climate Change Research 12(2), 281 (2021); https://doi.org/10.1016/j.accre.2021.03.004

[4] F. Wang et al. Sustainability 13(8), (2021); https://doi.org/10.3390/su13084580

[5] Y. Li et al. Structural Change and Economic Dynamics 53, 237 (2020); https://doi.org/10.1016/j.strueco.2020.02.007

[6] M. Ingaldi et al. Energies 13(24), (2020); https://doi.org/10.3390/en13246495

[7] Y. Li et al. Energy Policy 148, (2021); https://doi.org/10.1016/j.enpol.2020.111928

[8] W. Liu et al. Environ Sci Pollut Res Int 27(25), 31092 (2020); https://doi.org/10.1007/s11356-020-09470-0

[9] L. Pasquini et al. Progress in Energy 4(3), (2022).

[10] E. M. Dematteis et al. Progress in Energy 4(3), (2022).

[11] D. Prasad et al. Applied Surface Science 489, 538 (2019); https://doi.org/10.1016/j.apsusc.2019.06.041

[12] G. Bozkurt et al. Energy 180, 702 (2019); https://doi.org/10.1016/j.energy.2019.04.196

[13] O. Baytar. Acta Chim Slov 65(2), 407 (2018); https://doi.org/10.17344/acsi.2017.4151

[14] P. Martelli et al. J Phys Chem C 114(15), 7173 (2010); https://doi.org/10.1021/jp909341z

[15] K. Dileep et al. International Journal of Advancements in Research & Technology 2(7), 478 (2013).

[16] L. Z. Ouyang et al. Journal of Power Sources 269, 768 (2014); https://doi.org/10.1016/j.jpowsour.2014.07.074

[17] I. Dincer et al. International Journal of Hydrogen Energy 40(34), 11094 (2015); https://doi.org/10.1016/j.ijhydene.2014.12.035

[18] Y. Li et al. International Journal of Hydrogen Energy 45(17), 10433 (2020); https://doi.org/10.1016/j.ijhydene.2019.06.075

[19] N. P. Ghodke et al. International Journal of Hydrogen Energy 45(33), 16591 (2020); https://doi.org/10.1016/j.ijhydene.2020.04.143

[20] Z. Huang et al. International Journal of Hydrogen Energy 37(6), 5137 (2012); https://doi.org/10.1016/j.ijhydene.2011.12.033

[21] S. Ghosh et al. Applied Materials Today 20, (2020); https://doi.org/10.1016/j.apmt.2020.100693

[22] F. Wang et al. International Journal of Hydrogen Energy 44(26), 13185 (2019); https://doi.org/10.1016/j.ijhydene.2019.01.123

[23] B. Coşkuner Filiz et al. International Journal of Hydrogen Energy 44(53), 28471 (2019); https://doi.org/10.1016/j.ijhydene.2019.01.038

[24] C. Xu et al. Journal of Materials Chemistry A 6(29), 14380 (2018); https://doi.org/10.1039/C8TA03572E

[25] Y. Tonbul et al. J Colloid Interface Sci 553, 581 (2019); https://doi.org/10.1016/j.jcis.2019.06.038

[26] F. Zhong et al. International Journal of Hydrogen Energy 43(49), 22273 (2018); https://doi.org/10.1016/j.ijhydene.2018.10.064

[27] J. Li et al. Journal of the American Chemical Society 141(37), (2019).

[28] F. Fu et al. Journal of the American Chemical Society, (2018).

[29] J. Guo et al. Applied Catalysis B: Environmental 265, (2020); https://doi.org/10.1016/j.apcatb.2019.118584

[30] H. Jia et al. International Journal of Hydrogen Energy 43(43), 19939 (2018); https://doi.org/10.1016/j.ijhydene.2018.09.036

[31] Ö. Şahin et al. Journal of the Energy Institute 89(2), 182 (2016); https://doi.org/10.1016/j.joei.2015.02.005

[32] L. Wei et al. International Journal of Hydrogen Energy 43(3), 1529 (2018); https://doi.org/10.1016/j.ijhydene.2017.11.113

[33] G. Bozkurt et al. International Journal of Hydrogen Energy 43(49), 22205 (2018); https://doi.org/10.1016/j.ijhydene.2018.10.106

[34] Q. Miao et al. Journal of Materials Chemistry A 7(11), 5967 (2019).

[35] S. Akbayrak et al. ACS Sustainable Chemistry & Engineering 8(10), 4216 (2020); https://doi.org/10.1021/acssuschemeng.9b07402

[36] C. Saka et al. International Journal of Hydrogen Energy 45(30), 15086 (2020); https://doi.org/10.1016/j.ijhydene.2020.03.238

[37] D. G. Tong. RSC Advances 10(21), 12354 (2020); https://doi.org/10.1039/D0RA90028A

[38] C. Saka et al. International Journal of Hydrogen Energy 45(4), 2872 (2020); https://doi.org/10.1016/j.ijhydene.2019.11.199

[39] F. Wang et al. International Journal of Hydrogen Energy 43(18), 8805 (2018); https://doi.org/10.1016/j.ijhydene.2018.03.140

[40] Z. C. Fu et al. Chem Commun (Camb) 53(4), 705 (2017).

[41] M. Xu et al. Journal of Nanoparticle Research 20(12), (2018); https://doi.org/10.1007/s11051-018-4429-6

[42] Y. Wang et al. International Journal of Hydrogen Energy 45(16), 9845 (2020); https://doi.org/10.1016/j.ijhydene.2020.01.157

[43] M. S. İzgi et al. International Journal of Hydrogen Energy 41(3), 1600 (2016).

[44] X.-L. Zhang et al. Industrial & Engineering Chemistry Research 58(17), 7209 (2019).

[45] J. Li et al. Energy Storage Materials 27, 187 (2020); https://doi.org/10.1016/j.ensm.2020.01.011

[46] V. I. Simagina et al. Applied Catalysis A: General 394(1-2), 86 (2011); https://doi.org/10.1016/j.apcata.2010.12.028

[47] X. Wu et al. ACS Sustainable Chemistry & Engineering 6(7), 8427 (2018); https://doi.org/10.1021/acssuschemeng.8b00572

[48] C.-H. Liu et al. Applied Catalysis B: Environmental 91(1-2), 368 (2009); https://doi.org/10.1016/j.apcatb.2009.06.003

[49] K. Feng et al. Angew Chem Int Ed Engl 55(39), 11950 (2016); https://doi.org/10.1002/anie.201604021

[50] N. V. Lapin et al. Inorganic Materials 49(10), 975 (2013); https://doi.org/10.1134/S0020168513100063

[51] Y. Xu et al. Journal of Power Sources 261, 7 (2014); https://doi.org/10.1016/j.jpowsour.2014.03.038

[52] Y. Xu et al. International Journal of Hydrogen Energy 41(37), 16344 (2016); https://doi.org/10.1016/j.ijhydene.2016.05.234

[53] P. V. Ramachandran et al. Inorganic Chemistry 46(19), 7810 (2007); https://doi.org/10.1021/ic700772a

[54] L. Damjanović et al. Journal of Power Sources 195(10), 3284 (2010); https://doi.org/10.1016/j.jpowsour.2009.11.105

[55] M. S. İzgi et al. International Journal of Hydrogen Energy 45(60), 34857 (2020); https://doi.org/10.1016/j.ijhydene.2020.04.034

[56] Y. Wang et al. International Journal of Hydrogen Energy 44(21), 10508 (2019); https://doi.org/10.1016/j.ijhydene.2019.02.157

[57] M. Sait Izgi et al. Materials and Manufacturing Processes 34(14), 1620 (2019); https://doi.org/10.1080/10426914.2019.1594280

[58] M. Paladini et al. Applied Catalysis B: Environmental 158-159, 400 (2014); https://doi.org/10.1016/j.apcatb.2014.04.047

[59] Q. Xu et al. Journal of Power Sources 163(1), 364 (2006);

https://doi.org/10.1016/j.jpowsour.2006.09.043

[60] S. U. Jeong et al. Journal of Power Sources 144(1), 129 (2005); https://doi.org/10.1016/j.jpowsour.2004.12.046

[61] H. Çelik Kazici et al. Journal of Electronic Materials 49(6), 3634 (2020); https://doi.org/10.1007/s11664-020-08061-6

[62] H. Ç. Kazıcı et al. Journal of Electronic Materials 51(5), 2356 (2022); https://doi.org/10.1007/s11664-022-09491-0

[63] E. Onat et al. Journal of the Australian Ceramic Society 57(5), 1389 (2021); https://doi.org/10.1007/s41779-021-00643-9

[64] E. Onat et al. Journal of Materials Science: Materials in Electronics 32(23), 27251 (2021); https://doi.org/10.1007/s10854-021-07094-9

[65] C. Cui et al. Applied Catalysis B: Environmental 265, (2020); https://doi.org/10.1016/j.apcatb.2020.118612